A Strong Test of the Dark Matter Origin of a TeV Electron Excess Using IceCube Neutrinos

Yue Zhao[1a,b] **Ke Fang**[2c,d] **Meng Su**[3e] **M. Coleman Miller**[4c,d]

[a]Tsung-Dao Lee Institute, and Department of Physics and Astronomy, Shanghai Jiao Tong University, Shanghai 200240

[b]Leinweber Center for Theoretical Physics, University of Michigan, Ann Arbor, MI 48109

[c]University of Maryland, Department of Astronomy, College Park, MD, 20742

[d]Joint Space-Science Institute, College Park, MD, 20742

[e]Department of Physics and Laboratory for Space Research, the University of Hong Kong, PokFuLam, Hong Kong SAR, China

Abstract. Due to the electroweak symmetry, high energy neutrinos and charged leptons are generically produced simultaneously in heavy dark matter decay or annihilation process. Correlating these two channels in dark matter indirect detections may provide important information on the intrinsic production mechanism. In this paper, we demonstrate this point by studying the tentative excess in the electron spectrum at 1.4 TeV reported by the DArk Matter Particle Explorer (DAMPE). A non-astrophysical scenario in which dark matter particles annihilate or decay in a local clump has been invoked to explain the excess. If $e^{\pm}$ annihilation channels in the final states are mediated by left-handed leptons as a component in the $SU(2)_L$ doublet, neutrinos with similar energies should have been simultaneously produced. We demonstrate that generic dark matter models can be decisively tested by the existing IceCube data. In case of a non-detection, such models would be excluded at the 5σ level by the five-year data for a point-like source and by the ten-year data for an extended source of dark matter particles with left-handed leptons. This serves as an example of the importance of correlating charged lepton and neutrino channels. It would be fruitful to conduct similar studies related to other approaches to the indirect detection of dark matter.

---

[1]zhaoyhep@umich.edu

[2]kefang@umd.edu

[3]mengsu.astro@gmail.com

[4]miller@astro.umd.edu

Contents

1 Introduction

Correlating various channels in dark matter indirect detections is crucial to reduce the astrophysical uncertainties and extract information from the dark matter annihilation or decay processes.

TeV cosmic ray electrons (CRE) and neutrinos provide ideal probes of potential signatures of dark matter particle annihilation or decay in the vicinity of the solar system. TeV electrons cool very fast while propagating in the Milky Way, thus the sources of such high energy electrons must be within 1 kpc. The direction of the source is largely erased in the electron flux. On the other hand, the propagation of neutrinos is barely affected and provides excellent directional information. Furthermore, high energy neutrinos and charged leptons are generically correlated with each other due to the electroweak symmetry. If a hint of an excess is suggested in one channel, searching for the corresponding signal in the other channel can solidly test such a hypothesis.

The CRE spectrum has recently been directly measured up to 5 TeV using the spaceborne DArk Matter Particle Explorer (DAMPE; [1]). The DAMPE measurement of the CRE spectrum has unprecedented high energy resolution, low background, and well controlled instrumental systematics. Although the majority of the spectrum can be fitted by a smoothly broken power-law model with a spectral break at E$\sim$0.9 TeV, a tentative peak at $\sim$1.4 TeV in e^+e^- total spectrum has been claimed [2]. The excess of e^+e^- pairs at 1.4 TeV is approximately 2.5×10^{-8} GeV^{-1} s^{-1} sr^{-1} m^{-2} compared with the best continuum fit of the electron-positron energy spectrum of DAMPE [3]. Structures around TeV are also evident in the electron-positron spectrum measured by the Calorimetric Electron Telescope (CALET), although more statistics and refined data analysis are needed to reach a conclusion [4].

A sharp peak in the e^+e^- spectrum is hard to explain with a distant source. Electrons and positrons with TeV energy quickly lose energy via synchrotron radiation and inverse Compton scattering processes. Even if the initial spectrum is monoenergetic, propagation introduces a dispersion in the energy. If the peak is confirmed by future data, the 1.5% energy resolution of DAMPE in the TeV regime would require that the source of the TeV electrons and positrons has to be within 0.3 kpc [3, 5–20].

Two types of scenarios have been proposed to explain the DAMPE electron-positron flux. In an astrophysical scenario, an isolated young pulsar could produce such a sharp peak if it rotates relatively slowly and has a mild magnetic field (e.g., [3, 15]). In a non-astrophysical scenario, small dark matter (DM) substructure, such as a nearby clump, can produce a large e^+e^- flux due to its enhanced DM density (e.g., [7, 8]). It is thus crucial to explore correlated multi-messenger signals that may help to discriminate between possible explanations [5]. If an

association is established, the directional information carried by weakly-interacting particles such as neutrinos will be crucial to finding the source.

From a particle physics viewpoint, dark matter models fall into two generic groups according to the final state electron chirality. The left-handed electrons are fundamentally different from right-handed electrons. If the e^+e^- produced by DM are left-handed, one generically expects a comparable neutrino flux simultaneously. This is because the electroweak symmetry breaking (EWSB) scale is at O(100) GeV, thus induces negligible difference between left-handed electrons and neutrinos at an energy as high as 1.4 TeV. The associated neutrinos should be almost monochromatic and may carry important directional information if they come from a nearby DM clump.

In this work, using the $e^{\pm}$ flux at 1.4 TeV measured by DAMPE as a reference of the TeV electron excess, we illustrate that searching for associated neutrino signals can provide strong tests on DM interpretations. We first demonstrate that the accompanying neutrinos, with a monochromatic energy of 1.4 TeV, are naturally expected in a generic class of models. Then we briefly discuss the flavors of neutrinos when they reach the earth. Based on the neutrino background levels in the IceCube one-year public data, we demonstrate that the existing ∼8-year IceCube data is sufficient to decisively test the possibility that the DAMPE $e^{\pm}$ excess is left-handed and produced from the annihilation or decay of DM.

We emphasize that, in this paper, we use the tentative peak appearing in DAMPE's measurement as a demonstration to show the benefit on studying the correlation between electron and neutrino channels. We are not limited by this particular choice of benchmark scenario and similar studies can be applied in more general cases.

2   Classification of Models

If a left-handed electron is involved in the DM annihilation process, generically a comparable neutrino flux is also generated due to $SU(2)_L$ symmetry. We present a classification of models and demonstrate that a neutrino flux is naturally produced. To quantify the relative ratio, we define η_i as

$$\eta_i = L_{\nu_i}/L_e \tag{2.1}$$

where L is the injection luminosity and i labels the lepton flavor. We do not distinguish e^+ and e^- because they are indistinguishable using DAMPE at high energy. Similarly, IceCube data cannot distinguish neutrinos from anti-neutrinos. We have not yet included the effects of neutrino oscillation. If only electrons and positrons are produced, $\eta_{\mu,\tau} = 0$. For the flavor universal scenario, $\eta_{e,\mu,\tau}$ are all equal.

There are two ways to link dark matter with a standard model (SM) lepton: s or t-channel exchange of a mediator. Z' is a typical s-channel mediator, which is the gauge boson of a new $U(1)$ gauge group. Label the charges of left and right-handed leptons as $q'_{L,i}$ and $q'_{R,i}$, η_i is $\eta_i = q'^2_{L,i}/\left(q'^2_{L,e} + q'^2_{R,e}\right)$. If Z' does not couple to right handed leptons, then η_i is 1. With comparable charge assignments, η_i is O(1). In [21], the s-channel models were studied and we discuss the classification of the t-channel models in this section.

(i) $SU(2)_L$ singlet. If dark matter is a singlet of $SU(2)_L$ and the leptons in the final states are a $SU(2)_L$ doublet, the mediator should be an $SU(2)_L$ doublet,

$$L \supset \lambda_i \phi \Psi_{L,1} L_i + M_\Psi \Psi_{L,1} \Psi_{L,2} + h.c. \tag{2.2}$$

$\Psi_{L,1}$ and $\Psi_{L,2}$ are heavy vector-like fermions in the fundamental representation of $SU(2)_L$ with hypercharge +1 and -1. DM annihilation is mediated by Ψ. EWSB may introduce a mass splitting between $SU(2)_L$ components of Ψ. However EWSB happens around 100 GeV, much smaller than the hypothesized 1.4 TeV DM mass. The induced mass splitting is small, $< 10\%$, and comparable neutrino flux should be produced, i.e. $|1 - \eta_e| < 0.1$.

If DM is a real scalar, the leading annihilation is p-wave due to chirality suppression. Comparing with complex scalar DM, to achieve the same $e^+ e^-$ production rate, the DM energy density in the clump needs to be much larger, $O(\sim 10^3)$, assuming similar coupling constants and M_Ψ. DM particle may be fermionic. For a gauge singlet, it can pair with itself and form a Majorana fermion. DM can also be a Dirac fermion composed of two Weyl spinors. For Majorana DM, the dominant annihilation channel is again p-wave suppressed.

(ii) Non-trivial representation under $SU(2)_L$. Let us first consider the fundamental representation; we comment on higher representations later. If a DM particle is an $SU(2)_L$ doublet, the heavy mediator transforms under trivial or adjoint representation. We introduce two sets of Weyl spinors, χ_1 and χ_2, which are $SU(2)_L$ doublets with hypercharge +1 and -1. With a vector-like mass, their EM neutral components form a Dirac fermion as DM.

If the mediators, ϕ_n and ϕ_c, are $SU(2)_L$ singlets. They carry 0 and +2 hypercharge respectively. The Lagrangian is

$$L \supset \lambda_{1,i}\chi_1 L_i \phi_n + \lambda_{2,i}\chi_2 L_i \phi_c + M_\chi \chi_1 \chi_2 + m_n^2 \phi_n^2 + m_c^2 \phi_c^2 + h.c.$$

M_χ determines the DM mass scale. The relative ratio is determined by $\lambda_{1,i}$, $\lambda_{2,i}$ and $|m_{n,c}|$. With generic choices, $\eta_e \sim O(1)$.

η_e is a free parameter here because no symmetry relates $\lambda_{1,i}$, $\lambda_{2,i}$ and $|m_{n,c}|$. Such freedom is gone if the heavy mediator transforms non-trivially under $SU(2)_L$, e.g., an adjoint representation when DM is a doublet or when DM is in higher representation of $SU(2)_L$. Then η_e is expected to differ from unity by at most 10%.

In the $SU(2)_L$ doublet case, DM cannot be a Dirac fermion, because of strong dark matter direct detection constraints. Similar to the higgsinos in Minimal Supersymmetric Standard Model, a small mixing after EWSB with other fermions, such as the Wino or Bino, breaks a Dirac fermion into two Majorana fermions. The DM direct detection constraints can then be evaded. Since DM is effectively Majorana, its annihilation is p-wave suppressed.

We now comment briefly on the DM decay which can be realized when mediators are lighter than DM. The lifetime of the dark matter particle can be cosmologically long if the coupling between the DM field and the mediator is very weak. This can be naturally realized if such vertex violates an approximate global symmetry. The energy of the electron and neutrino is

$$E_{e,\nu} = \frac{m_{DM}^2 - m_{med}^2}{2m_{DM}} \tag{2.3}$$

Some components of the mediator are charged, but the collider constraints are weak. If the heavy charged particles are long-lived, their mass can still be O(100) GeV [22, 23]. The charged heavy particles may lose its charge by decaying to charged SM leptons and neutral particles. This evades potential problems in cosmology. The charged leptons from the secondary decay is softer and can hide in the continuous cosmic-ray background.

Neutrino Oscillation The flavor of a neutrino changes during propagation. We present the detailed calculation for neutrino oscillations in the Appendix. For a sizable DM clump considered here, i.e., O(10) pc, the observed neutrino fraction, κ_i, is independent on the DM

clump size and the distance to us as shown in Figure 2. In the Appendix, we show the flavor fraction in two scenarios, electron-only and flavor universal. The undetermined CP violating angle in PMNS matrix δ_{CP} only affects the results by O(1), thus it does not change our conclusion qualitatively.

3 Neutrino Flux

After leaving a source, TeV electrons diffuse in the Galactic magnetic field while neutrinos travel in a straight path to reach the earth. We now describe how the electron and the neutrino fluxes are connected.

The density of particles n at a location $\vec{x}$ from a source at $\vec{x}_s$ follows the transport equation [25]

$$\frac{\partial n(\vec{x}, E)}{\partial t} = D(E) \nabla^2 n + Q_s(E)\delta(\vec{x} - \vec{x}_s) \,, \tag{3.1}$$

assuming that there is no energy loss and that the source is stationary. Here $D(E) = D_0 \, (E/E_0)^\alpha$ is the spatial diffusion coefficient, with $D_0 = 10^{28}\, \mathrm{cm^2\, s^{-1}}$, $\alpha = 1/3$ and $E_0 = 3$ GeV corresponding to the diffusion coefficient in the interstellar medium [25], and $Q_s(E)$ is the particle injection rate. The solution can be written as [1]

$$n_e(E) = \frac{Q_e(E)}{4\pi\, R_s\, D(E)} \tag{3.2}$$

Assuming that the DAMPE excess is due to a monochromatic electron population with an observed energy density $w_e = n_e\, E_e = 9.8 \times 10^{-19}\, \mathrm{erg\, cm^{-3}}$ [3], the electron injection power is $L_e = 7.6 \times 10^{32}\, (R_s/0.2\,\mathrm{kpc}) \left(D(E)/10^{29}\,\mathrm{cm^2\, s^{-1}}\right)\, \mathrm{erg\, s^{-1}}$.

A population of neutrinos is produced at the same time as the electrons. The injection powers of the two species are connected by Eq. 2.1. The neutrino flux is then

$$\begin{aligned} F_{\nu_j} &= \frac{\sum_i \eta_i\, \kappa_j\, L_e}{\delta\left(\log E_\nu\right)\, 4\pi\, R_s^2} \tag{3.3} \\ &= 8.3 \times 10^{-8}\, \eta\, \left(\frac{R_s}{0.2\,\mathrm{kpc}}\right)^{-1} \left(\frac{D(E)}{10^{29}\,\mathrm{cm^2\, s^{-1}}}\right) \\ &\quad \left(\frac{\sigma\left(\log E_\nu\right)}{1.2}\right) \left(\frac{\sum_i \eta_i\, \kappa_j}{1}\right)\, \mathrm{GeV\, cm^{-2}\, s^{-1}} \end{aligned}$$

where $\delta\left(\log E_\nu\right)$ is the energy resolution of neutrino events, which is $\delta\left(\log E_{\nu_\mu}\right) \sim 1.2$ for the IceCube ν_μ events based on the reconstruction of the muon energy in the IceCube detector [24]. κ_i is the fraction of neutrino in each flavor at the time of detection. More details about neutrino oscillation can be found in the Appendix.

The neutrino flux depends on the source distance. A DM clump with a total mass of $10^7 - 10^8\, M_\odot$ with a distance of $0.1 - 0.3\,\mathrm{kpc}$ has been suggested to account for the DAMPE TeV data [3]. The source is unlikely to be more distant than O(1) kpc, as electrons would have suffered from significant energy loss and not present a feature as narrow as in the DAMPE spectrum. We thus choose $0.2\,\mathrm{kpc}$ as a default distance for the following calculations.

---

[1] When there is more than one DM clump nearby, our calculation would still apply if a single clump makes the dominant contribution to the electron and neutrino fluxes.
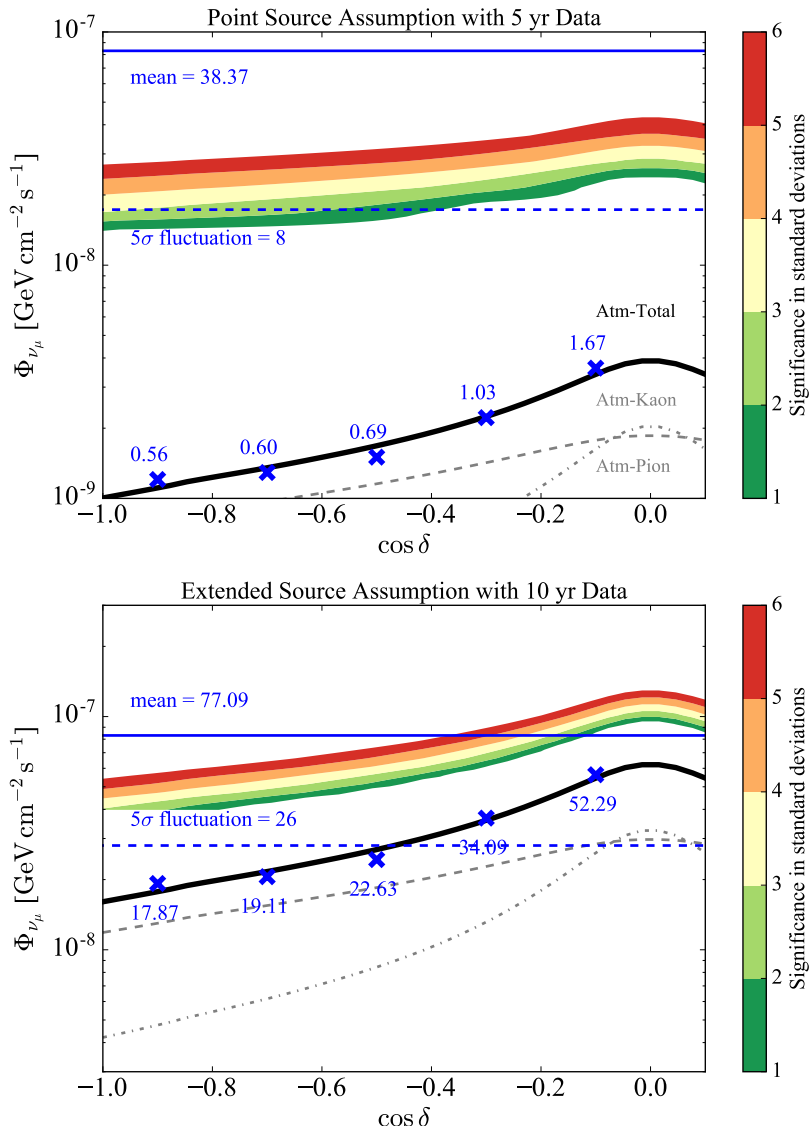
Figure 1. The flux of neutrinos from a fiducial dark matter source that may produce the 1.4 TeV excess in the electron spectrum measured using DAMPE (mean and a hypothetical 5σ downward fluctuation in blue lines), compared with the flux of the atmospheric neutrino background around 1.4 TeV (kaon and pion components are indicated by grey dash-dotted and dashed lines, and the total is shown by the black solid line). The top and bottom panels assume that the source is point-like and extended respectively. In the top (bottom) panel, the blue cross data points present the average number of TeV events in a $0.5° \times 0.5°$ ($2° \times 2°$) sky patch in the five-year (ten-year) IceCube data, which is obtained by scaling that in the IceCube-86 2011-2012 data by the corresponding number of years [24]. The colored contours show the flux needed for the source to stand out of the atmospheric background with 1 to 6σ significance levels. We find that the existing $\sim$8-year IceCube data can decisively test a generic class of dark matter models that produce neutrinos and the DAMPE TeV electrons simultaneously.

For comparison, at 1.4 TeV, the averaged conventional muon neutrino flux per solid

angle, including both pion and kaon contributions, is $3 \times 10^{-5} \, \mathrm{GeV \, cm^{-2} \, s^{-1} \, sr^{-1}}$ [26]. The averaged conventional electron neutrino flux per solid angle is $2 \times 10^{-6} \, \mathrm{GeV \, cm^{-2} \, s^{-1} \, sr^{-1}}$ [26]. If the observed electrons arrive from a preferred direction, which for example may be indicated by an anisotropy in the electron data, one can search for coincident neutrinos in the associated sky location. The average angular resolution of the IceCube detector is $0.5°$ for ν_μ events and a few degrees for ν_e events at ~ 1 TeV. The background flux in the sky patch surrounding the source direction would thus be $F_{\nu_\mu}^{\mathrm{bg}} = 2.3 \times 10^{-9} \, (\delta\theta/0.5°)^2 \, \mathrm{GeV \, cm^{-2} \, s^{-1}}$ and $F_{\nu_e}^{\mathrm{bg}} = 1.5 \times 10^{-8} \, (\delta\theta/5°)^2 \, \mathrm{GeV \, cm^{-2} \, s^{-1}}$

Using the IceCube effective area of $\sim 5000 \, \mathrm{cm^2}$ at 1.4 TeV, Eq. 3.3 corresponds to an average of 7.7 events per year of IceCube data. Therefore it will be easy to use IceCube to identify a bright source if we know its location in the sky. However, no specific directional information has been provided by the current data of DAMPE [1]. This could be due to a limit of the statistics, or because electrons started from a relatively distant location and have lost most of their angular information during a diffusive propagation. Below we investigate the feasibility of a blind search for the associated neutrino signal using the IceCube muon neutrinos events. We do not use cascade events due to their poor angular resolutions, but note that they may be useful for searches for very extended sources as shown in Ref. [27].

We analyze the public IceCube data from the full 86-string detector configuration taken during 2011-2012, using only up-going neutrinos from the northern sky to eliminate background muon events [24]. The sample contains a total of 20,145 neutrino events with reconstructed energy in the approximate 320 GeV to 20 TeV range. We select 18,722 events that may have a deposition energy at 1.4 TeV according to a $\delta \left(\log E_{\nu_\mu} \right) \sim 1.2$ energy resolution [24] (between 320 GeV and 3080 GeV). The public data only have the zenith angle of the reconstructed events, rather than the full two-dimensional angular location, so we cannot perform an analysis with these data alone. In the following, however, we project an analysis based on an extrapolation of the neutrino numbers to a 5-year and a 10-year data set, which we assume will include both the zenith angle and the azimuthal angle for each reconstructed event.

The events are pixelized based on a HEALPix71 [28] pixelization scheme for spatial binning. Two source scenarios are considered. In the first scenario, we assume that the dark matter source is point-like. We choose a bin size of approximately $0.5° \times 0.5°$ (with the HEALPix parameter Nside = 128, corresponding to the angular solution of the IceCube ν_μ events [24]. In the second scenario, we assume that the source is extended. We choose a spatial bin size of $\sim 2° \times 2°$ (Nside = 32), corresponding to a dark matter clump with a size of $\sim 10 \, \mathrm{pc}$ and a distance of $\sim 0.2 - 0.3 \, \mathrm{kpc}$ as suggested for e.g. by the benchmark case in Ref. [3]. We divide the data into 6 bins according to the zenith angle of the reconstructed events, and let all bins have equal solid angles. We verify that the event number in pixels in all zenith angle bands follows the Poisson distribution.

Figure 1 presents the flux of TeV neutrinos from the atmospheric background in an element sky patch (a pixel in our analysis) in the point-source and the extended-source scenarios, comparing to the flux of neutrinos from a fiducial source that produces the DAMPE TeV electrons. The solid black line corresponds to the atmospheric model of [26], including both pion and kaon components. The blue cross data points and their values show the average number of events in a pixel at the corresponding zenith angle expected in five-year data (top) and ten-year data (bottom). The values are obtained by scaling the average event number in one pixel in the 2011-2012 data by the number of observational years. The dependence of the event number on the zenith angle is consistent with that of the total atmospheric

neutrino flux. The scaling between the two is obtained by fitting the data to the model, and its physical meaning is the effective area multiplied by the observational time and the angular size of the pixel. The colored contours show the flux levels that are needed to reach a 1 to 6 σ deviation from a background-only hypothesis. Specifically, the local probability of deviation is calculated using the Poisson distribution with a mean determined by the average number of atmospheric neutrinos in a pixel. The local probability is then corrected by a trial factor that equals to the number of independent pixels used in the analysis. Finally, the global probability is quoted using the corresponding number of standard deviations for a Gaussian distribution.

The solid blue line indicates the expected number of neutrino events from a dark matter source that may explain the TeV excess of electrons measured by DAMPE (as described by equation 3.3). We find that in both point-source and extended source scenarios, the mean flux is high enough to reject a background-only hypothesis with high significance. We additionally consider a pessimistic scenario in which the number of neutrino events from the dark matter source is 5-σ below its mean value, integrated over the uncertainty of the DAMPE electron flux at 1.4 TeV, as indicated by the dashed blue line in both plots. Even in this case, the five-year data is able to reveal a dark matter source in most part of the northern sky with high confidence levels.

4 Conclusion

In this letter, we demonstrate the feasibility of testing TeV dark matter models by neutrino observations. We focus on a benchmark scenario in which the tentative TeV electron excess measured by DAMPE is explained by the DM annihilation or decay in a nearby subhalo. In a generic class of dark matter models where $e^{\pm}$ from DM annihilation or decay are in a $SU(2)_L$ doublet, neutrinos of comparable flux are simultaneously generated. We have shown that the existing $\sim$8-year IceCube data is sufficient to identify the associated neutrinos with high significance, and decisively test any dark matter models using left-handed leptons to explain the DAMPE TeV peak.

For a point-like subhalo in the northern sky, our results are robust even in a pessimistic scenario where due to fluctuations the neutrino flux is 5σ lower than expected. For an extended source, ten years of IceCube data can reveal its existence in most parts of the northern sky. But if the source is much more extended than an angular size of $\sim 2°$, the prospects for using IceCube to detect or constrain the dark matter source would not be as good. We do note that there are two refinements to our analysis that could improve those prospects significantly. First, we assumed for simplicity that the neutrino flux from an extended source would be uniform over the whole solid angle. In reality, the flux would be centrally concentrated in a way specific to the halo properties, so a search for that concentration would yield a stronger signal. Second, we likewise assumed that the reconstructed background atmospheric neutrino flux is equally spread over the entire $\sim 300 - 3000$ GeV range, but in fact that flux drops sharply with increasing energy. As a result, the excess signal at higher reconstructed energies is likely to be substantially larger than in our current conservative estimates.

The propagation of electrons depends on the diffusion coefficient of the region between the source and the earth. If the diffusion coefficient is well below the average value of the ISM (as it is in the region surrounding the Geminga pulsar [29, 30]), electrons would be confined to be near the source for longer. To maintain a non-broadened peak feature, the
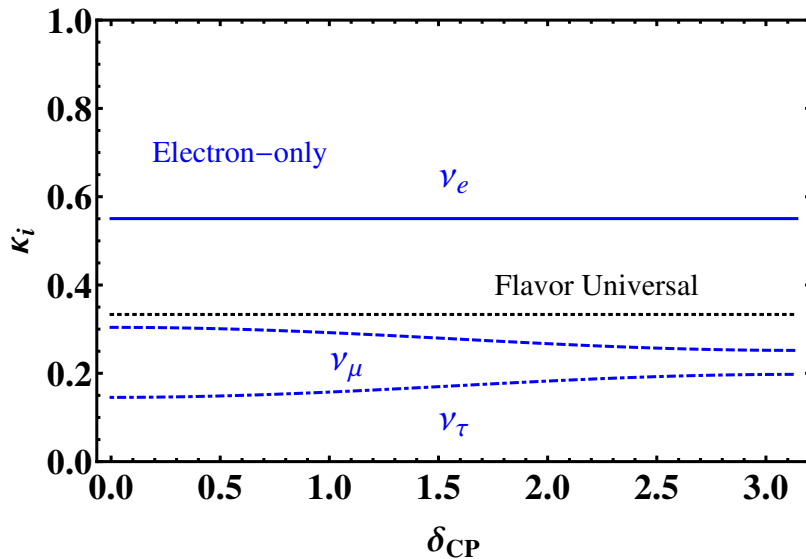
Figure 2. The fraction of each flavor in the measured neutrino flux around the earth. The blue lines correspond to the scenario in which only electron neutrinos are produced by DM annihilation. Solid, dashed and dot-dashed lines are for electron, muon and tau neutrinos respectively. The black dotted line is for the flavor universal scenario, in which the fractions for each flavor is equal to 1/3.

source would then need to be closer than that in our benchmark case. Therefore the neutrino flux (in equation 3.3) does not strongly depend on the diffusion coefficient.

We have used the IceCube detector to test DM models in this work. Other high-energy neutrino experiments, including the Super-Kamiokande [31] and the ANTARES Telescope [32] may provide additional sky coverages to find or constrain associated neutrino signals. Future experiments such as IceCube-Gen2 [33] and KM3NeT [34] will provide improved sensitivity to examine very extended or extremely faint dark matter halos.

Neutrino oscillations and injection channels

Mixing among neutrinos can be characterized by the PMNS matrix, U. Neglecting the possible CP phases from the Majorana mass terms, there are four parameters in PMNS matrix: three mixing angles and one CP phase, i.e. $\{\theta_{12}, \theta_{13}, \theta_{23}, \delta_{CP}\}$. θ_{12} and θ_{13} have been measured with good accuracy, $\sin^2(2\theta_{13}) = 0.093 \pm 0.008$ and $\sin^2(2\theta_{12}) = 0.846 \pm 0.021$. θ_{23} has larger uncertainty, $\sin^2(2\theta_{23}) > 0.92$. In the following calculation, we take the central values of $\sin^2(2\theta_{12})$ and $\sin^2(2\theta_{13})$, while $\sin^2(2\theta_{23})$ is taken to be 0.97. The uncertainties in these values do not change our results qualitatively. δ_{CP} remains to be determined, and we treat it as a free parameter.

The oscillation of neutrinos is then written as

$$P_{\alpha \to \beta} = \delta_{\alpha\beta} - 4 \sum_{i>j} Re(U_{\alpha i}^* U_{\beta i} U_{\alpha j} U_{\beta j}^*) \sin^2 \left(\frac{\Delta m_{ij}^2 L}{4E} \right)$$

$$+ \ 2 \sum_{i>j} Im(U_{\alpha i}^* U_{\beta i} U_{\alpha j} U_{\beta j}^*) \sin \left(\frac{\Delta m_{ij}^2 L}{4E} \right) \tag{4.1}$$

Here Δm_{ij}^2 is the mass square splitting among neutrino mass eigenstates. In a vacuum, $\Delta m_{21}^2 = (7.53 \pm 0.18) \times 10^{-5} \text{eV}^2$ and $|\Delta m_{31}^2| \simeq |\Delta m_{32}^2| = (2.44 \pm 0.06) \times 10^{-3} \text{eV}^2$. The size of the DM clump which generates the monochromatic electron flux can be large, for example O(10) pc as considered in our benchmark case. For neutrinos with energy O(TeV), this is much larger than the distance to have one oscillation, i.e. $\left(\frac{\Delta m_{ij}^2 10\text{pc}}{4\text{TeV}} \right) \gg 1$. After averaging the whole clump,

$$\langle P_{\alpha \to \beta} \rangle = \delta_{\alpha\beta} - 2 \sum_{i>j} Re(U_{\alpha i}^* U_{\beta i} U_{\alpha j} U_{\beta j}^*) \tag{4.2}$$

(a) Electron-only channel: this is the scenario where DM annihilation only produces electrons and electron neutrinos. The flavor fraction of neutrino flux, κ_i, are labeled as blue lines in Fig. 1.

(b) Flavor-universal channel: if the DM annihilation is universal in flavor, i.e. the initial flux for each flavor is the same, the flux observed on earth remains flavor universal, guaranteed by the unitarity of the mixing matrix. This is represented by the black dotted line in Fig. 1.

Acknowledgements

References

[1] J. Chang, G. Ambrosi, Q. An, R. Asfandiyarov, P. Azzarello, P. Bernardini et al., *The DArk Matter Particle Explorer mission*, *Astroparticle Physics* **95** (Oct., 2017) 6–24, [arXiv:1706.08453].

[2] DAMPE collaboration, G. Ambrosi et al., *Direct detection of a break in the teraelectronvolt cosmic-ray spectrum of electrons and positrons*, arXiv:1711.10981.

[3] Q. Yuan et al., *Interpretations of the DAMPE electron data*, arXiv:1711.10989.

[4] O. Adriani, Y. Akaike, K. Asano, Y. Asaoka, M. G. Bagliesi, G. Bigongiari et al., *Energy Spectrum of Cosmic-Ray Electron and Positron from 10 GeV to 3 TeV Observed with the Calorimetric Electron Telescope on the International Space Station*, *Physical Review Letters* **119** (Nov., 2017) 181101, [arXiv:1712.01711].

[5] Y. Gao and Y.-Z. Ma, *Dark matter cascade decay implications from DAMPE, HESS, Fermi-LAT and AMS02*, *ArXiv e-prints* (Nov., 2017) , [arXiv:1712.00370].

[6] W. Chao, H.-K. Guo, H.-L. Li and J. Shu, *Electron Flavored Dark Matter*, *ArXiv e-prints* (Nov., 2017) , [arXiv:1712.00037].

[7] X. Liu and Z. Liu, *TeV dark matter and the DAMPE electron excess*, *ArXiv e-prints* (Nov., 2017) , [arXiv:1711.11579].

[8] G. H. Duan, X.-G. He, L. Wu and J. M. Yang, *Leptophilic dark matter in gauged $U(1)\_L\_e - L\_\mu$ model in light of DAMPE cosmic ray $e^+ + e^-$ excess*, *ArXiv e-prints* (Nov., 2017) , [arXiv:1711.11563].

[9] J. Cao, L. Feng, X. Guo, L. Shang, F. Wang and P. Wu, *Scalar dark matter interpretation of the DAMPE data with U(1) gauge interactions*, *ArXiv e-prints* (Nov., 2017) , [arXiv:1711.11452].

[10] P. Athron, C. Balazs, A. Fowlie and Y. Zhang, *Model-independent analysis of the DAMPE excess*, *ArXiv e-prints* (Nov., 2017) , [arXiv:1711.11376].

[11] P.-H. Gu, *Radiative Dirac neutrino mass, DAMPE dark matter and leptogenesis*, *ArXiv e-prints* (Nov., 2017) , [arXiv:1711.11333].

[12] W. Chao and Q. Yuan, *The electron-flavored Z'-portal dark matter and the DAMPE cosmic ray excess*, *ArXiv e-prints* (Nov., 2017) , [arXiv:1711.11182].

[13] Y.-Z. Fan, W.-C. Huang, M. Spinrath, Y.-L. Sming Tsai and Q. Yuan, *A model explaining neutrino masses and the DAMPE cosmic ray electron excess*, *ArXiv e-prints* (Nov., 2017) , [arXiv:1711.10995].

[14] H.-B. Jin, B. Yue, X. Zhang and X. Chen, *Cosmic ray e^+e^- spectrum excess and peak feature observed by the DAMPE experiment from dark matter*, *ArXiv e-prints* (Nov., 2017) , [arXiv:1712.00362].

[15] I. Cholis, T. Karwal and M. Kamionkowski, *Features in the Spectrum of Cosmic-Ray Positrons from Pulsars*, *ArXiv e-prints* (Nov., 2017) , [arXiv:1712.00011].

[16] X.-J. Huang, Y.-L. Wu, W.-H. Zhang and Y.-F. Zhou, *Origins of sharp cosmic-ray electron structures and the DAMPE excess*, *ArXiv e-prints* (Nov., 2017) , [arXiv:1712.00005].

[17] L. Zu, C. Zhang, L. Feng, Q. Yuan and Y.-Z. Fan, *Constraints on box-shaped cosmic ray electron feature from dark matter annihilation with the AMS-02 and DAMPE data*, *ArXiv e-prints* (Nov., 2017) , [arXiv:1711.11052].

[18] Q. Yuan, L. Feng, P.-F. Yin, Y.-Z. Fan, X.-J. Bi, M.-Y. Cui et al., *Interpretations of the DAMPE electron data*, *ArXiv e-prints* (Nov., 2017) , [arXiv:1711.10989].

[19] K. Fang, X.-J. Bi and P.-F. Yin, *Explanation of the knee-like feature in the DAMPE cosmic $e^- + e^+$ energy spectrum*, *ArXiv e-prints* (Nov., 2017) , [arXiv:1711.10996].

[20] F. Yang and M. Su, *Dark Matter Annihilation from Nearby Ultra-compact Micro Halos to Explain the Tentative Excess at 1.4 TeV in DAMPE data*, [arXiv:1712.01724].

[21] P. Athron, C. Balazs, A. Fowlie and Y. Zhang, *Model-independent analysis of the DAMPE excess*, [arXiv:1711.11376].

[22] ATLAS collaboration, G. Aad et al., *Searches for heavy long-lived charged particles with the ATLAS detector in proton-proton collisions at $\sqrt{s} = 8$ TeV*, *JHEP* **01** (2015) 068, [arXiv:1411.6795].

[23] CMS collaboration, V. Khachatryan et al., *Search for long-lived charged particles in proton-proton collisions at $\sqrt{s} = 13TeV$*, *Phys. Rev.* **D94** (2016) 112004, [arXiv:1609.08382].

[24] M. G. Aartsen, K. Abraham, M. Ackermann, J. Adams, J. A. Aguilar, M. Ahlers et al., *Searches for Sterile Neutrinos with the IceCube Detector*, *Physical Review Letters* **117** (Aug., 2016) 071801, [arXiv:1605.01990].

[25] V. S. Berezinskii, S. V. Bulanov, V. A. Dogiel and V. S. Ptuskin, *Astrophysics of cosmic rays*. 1990.

[26] T. K. Gaisser and M. Honda, *Flux of atmospheric neutrinos*, *Annual Review of Nuclear and Particle Science* **52** (2002) 153–199, [arXiv:hep-ph/0203272].

[27] IceCube Collaboration, M. G. Aartsen, M. Ackermann, J. Adams, J. A. Aguilar, M. Ahlers et al., *Search for astrophysical sources of neutrinos using cascade events in IceCube*, *ArXiv e-prints* (May, 2017) , [arXiv:1705.02383].

[28] K. M. Górski, E. Hivon, A. J. Banday, B. D. Wandelt, F. K. Hansen, M. Reinecke et al., *HEALPix: A Framework for High-Resolution Discretization and Fast Analysis of Data Distributed on the Sphere*, *ApJ* **622** (Apr., 2005) 759–771, [`arXiv:astro-ph/0409513`].

[29] D. Hooper, I. Cholis, T. Linden and K. Fang, *HAWC observations strongly favor pulsar interpretations of the cosmic-ray positron excess*, *PRD* **96** (Nov., 2017) 103013, [`arXiv:1702.08436`].

[30] A. U. Abeysekara, A. Albert, R. Alfaro, C. Alvarez, J. D. Álvarez, R. Arceo et al., *Extended gamma-ray sources around pulsars constrain the origin of the positron flux at Earth*, *ArXiv e-prints* (Nov., 2017) , [`arXiv:1711.06223`].

[31] E. Richard, K. Okumura, K. Abe, Y. Haga, Y. Hayato, M. Ikeda et al., *Measurements of the atmospheric neutrino flux by Super-Kamiokande: Energy spectra, geomagnetic effects, and solar modulation*, *PRD* **94** (Sept., 2016) 052001, [`arXiv:1510.08127`].

[32] ANTARES Collaboration, A. Albert, M. André, M. Anghinolfi, G. Anton, M. Ardid et al., *The ANTARES Collaboration: Contributions to ICRC 2017 Part III: Searches for dark matter and exotics, neutrino oscillations and detector calibration*, *ArXiv e-prints* (Nov., 2017) , [`arXiv:1711.01496`].

[33] IceCube-Gen2 Collaboration, :, M. G. Aartsen, M. Ackermann, J. Adams, J. A. Aguilar et al., *IceCube-Gen2: A Vision for the Future of Neutrino Astronomy in Antarctica*, *ArXiv e-prints* (Dec., 2014) , [`arXiv:1412.5106`].

[34] S. Adrián-Martínez, M. Ageron, F. Aharonian, S. Aiello, A. Albert, F. Ameli et al., *Letter of intent for KM3NeT 2.0*, *Journal of Physics G Nuclear Physics* **43** (Aug., 2016) 084001, [`arXiv:1601.07459`].